Geotechnical, mineralogical, chemical and mechanical characterization of clay raw material from Korona (Burkina Faso) used in pottery.

Mohamed Seynou[1*], Raguilnaba Ouedraogo[1], Younoussa Millogo[1,2], Karfa Traoré[1], Beyon C. A. Bama[1]

[1]Laboratoire de Physico-Chimie et de Technologie des Matériaux, Unité de Formation en Sciences Exactes et Appliquées, Université de Ouagadougou, 03 BP : 7021 Ouagadougou 03, Burkina Faso.
[2]Institut des Sciences de la Nature et de la Vie (ISNV), Université Polytechnique de Bobo-Dioulasso,01 BP 1091 Bobo 01, Burkina Faso..

(Reçu le 14/09/2008 – Accepté après corrections le 12/05/2009)

Summary: A raw clayey material deposits from Korona (Burkina Faso) used in pottery was studied for industrial using. The geotechnical tests conducted on this raw material showed that this one is plastic. The X-ray diffraction and the chemical analyses showed that this raw clayey material is mainly constituted of kaolinite (37wt.%) and quartz (18wt.%), and minor contents of orthose (17wt.%), albite (13wt.%), talc (4wt.%) and calcite (2wt.%). These three latter compounds are responsible of good physico-chemical and mechanical properties of the studied material. The tiles elaborated with this raw material without any additive are characterised by feeble porosity (0.69%) and high flexural strength (59.5MPa) at 1150°C. These tiles are suitable according to the standards for habitats because of their physical and mechanical properties.
Keywords: Clay, Mineralogy, Physical and Mechanical Properties, Ceramic.

Caractérisation géotechnique, minéralogique, chimique et mécanique d'un matériau argileux de Korona (Burkina Faso) utilisé en poterie.

Résumé : Un matériau argileux en provenance de Korona (Burkina Faso) utilisé en poterie a été étudié pour une utilisation industrielle. Les tests géotechniques montrent que le matériau est une argile de plasticité moyenne. Les principales phases cristallines identifiées par couplage de l'analyse chimique et de la diffraction des rayons x sont la kaolinite (37%) et le quartz (18%). La présence d'autres éléments tels que le feldspath (orthose 17%, albite 13%), le talc (4%) et la calcite (2%) confère au matériau d'intéressantes propriétés physico-chimiques. Les propriétés mécaniques des produits céramiques issus du matériau sont intéressantes. A 1150°C, la faible porosité (0,69%) et le module de rupture élevé (59,5MPa) confèrent au matériau une utilisation dans la production du carreau de sol. La composition chimique du matériau combinée aux propriétés mécaniques justifie une possibilité d'utilisation potentielle de notre matériau en céramique industrielle sans ajouts.

Mots clés : Argile, Minéralogie, Propriétés Physique et Mécanique, Céramique.

[*] Corresponding author: Tel: +226 76 59 60 74; E-mail address: *seynou1mohamed@yahoo.fr*

1. Introduction

Many studies have shown that subsoil of Burkina Faso is rich in clayey minerals. Pottery constituted the principal application of these clayey minerals during many decades. In the last years, ceramics industries like CERAMIX (tiles manufacturing) and POCERAM (porcelains manufacturing) are slowly developed. In spite of this wealth of clay raw materials, the ceramics factories import (Spain) some raw materials. This situation which weakens the companies' management is undeniably due to the inexistence of scientist data on clayey materials deposit in Burkina Faso.

Indeed, few studies [1-4] were undertaken on some materials of Burkina Faso in order to resolve this problem.

The aim of this work is a contribution on the study of a clayey material from Burkina Faso in order to evaluate its suitability for tiles. For this purpose, chemical, mineralogical by X-ray diffraction (XRD), infra-red spectroscopy (IR), differential thermal analysis and scan electronic microscopy (SEM) were used. Physical and mechanical properties such as flexural strength, porosity and the linear shrinking of sintered tiles were determinated.

2. Raw material and experimental methods

The studied raw material deposit is from Korona (Banfora): 10°43' North and 5°04' West (**Fig.1**). The material is widely used by the local populations for their pottery activities.

The particle size distribution has been achieved according to NF P 94 – 057 standard [5].The liquid limit was measured by the method of the disc of Casagrande (W_L) and the plastic limit by the roller method (W_P). All these measures were performed according to NF P 94 - 051 standard [6].

X-rays diffraction of the powder was recorded with a diffractometer Brüker D 5000 with back graphite monochromator using CuKα radiation and functioning at 40Kv and 50mA. The diffractograms were treated with Diffracplus D Quant software.

The infrared spectrum of the sample was obtained with a Perkin Elmer FT- IR spectrometer in the range 400 and 4000 cm^{-1}. The sample (5mg) was mixed with 500mg of potassium bromide (KBr) and pressed into disc using 5tonnes as pressure for 5min followed by 10 tonnes as pressure for 5min.

The DTA/TGA of the crushed sample (< 100µm) was obtained using a Linseis instrument, operating at 5°C/mn from ambient temperature to 1200°C. Oxide alumina is taken as reference.

A Hitachi S2500 scanning electron microscope produced the SEM image. The powder of the sample was dispersed in an ultrasound bath for 1h. Suspension droplets were placed on a metal plate and allowed to evaporate slowly. Then they were coated with gold metal.

For the chemical composition determination, the ground sample (80µm) was etched by a mixture of sulfo-nitric and hydrochloric acid according to Njopwouo's protocol [7] and analyzed by atomic absorption spectrometry, using a Perkin Elmer A Analyst 100, colorimetry using a UV-visible Safas Double Energy Systeme spectrometer and gravimetry.

For the elaboration of specimen (10cmx4cmx1cm), crushed raw material (<63µm) was humidified (average 5wt.%) and pressed at 15MPa. The obtained bars are dried for 24h at 110°C, and fired at soaking varying from (950-1100°C) for 45min. The heating rate was 10°C/min. The technological properties measured on the fired tiles were: water absorption, linear shrinkage and flexural strength. The porosity of the material at the different temperatures was characterized by water absorption during immersion of product during 2 hours. The flexural strength σ was calculated with the equation $\sigma = \frac{3.F.E}{2.l.e^2}$ (F: applied force, E: distance

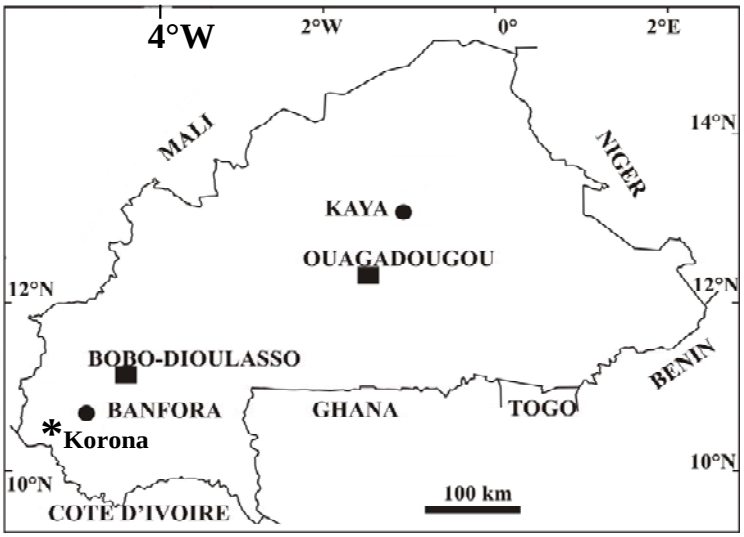

Figure 1: Location of Korona on the map of Burkina Faso

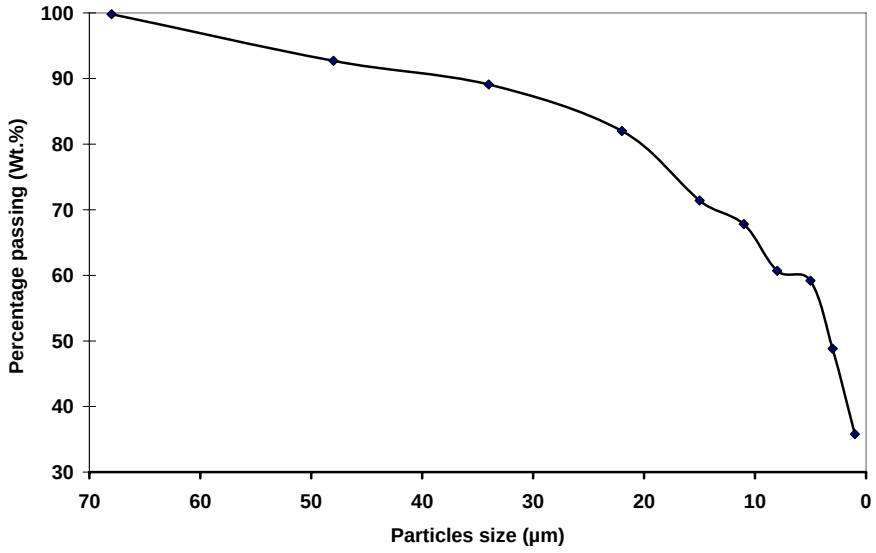

Figure 2: Particle size distribution curve of the sample

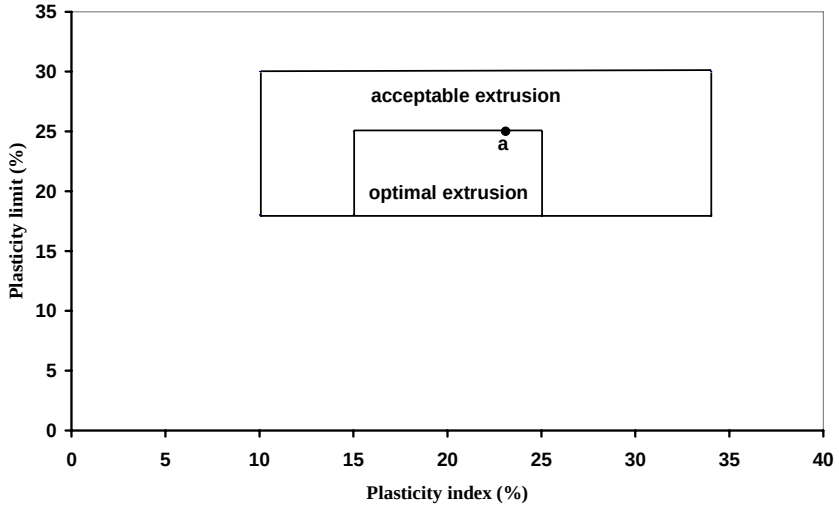

Figure 3: Marsigli Diagram through Atterberg limits: (•a location of the sample)[9]

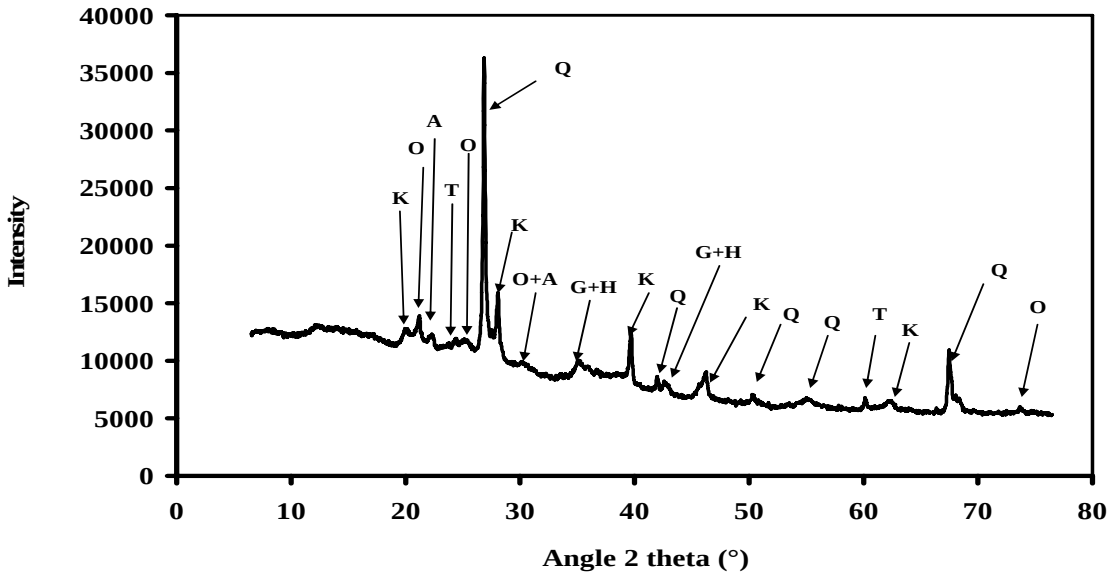

K: kaolinite, Q: quartz, O: orthoclase, A: albiteG: goéthite, H: hematite, T: talc, C: calcite

Figure 4: Powder x-ray diffraction pattern of the studied sample

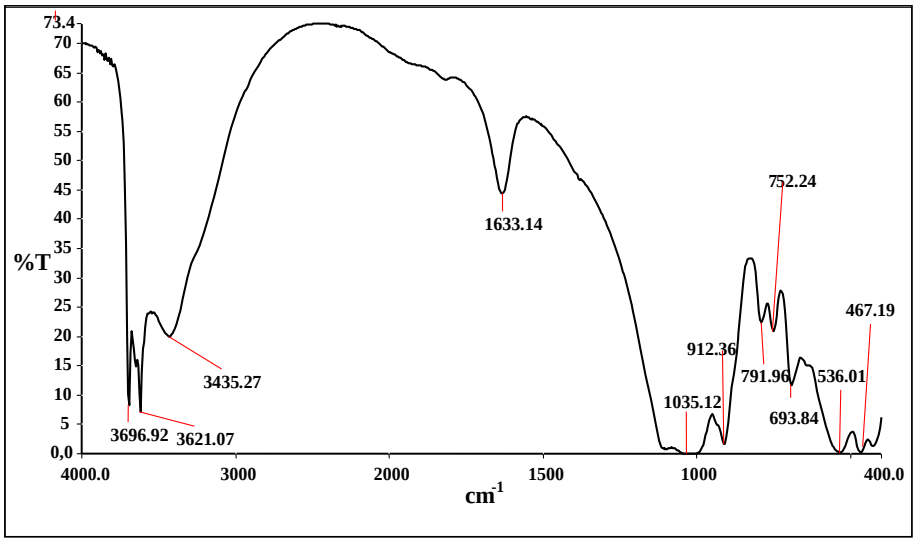

Figure 5: Infrared spectrum of the studied sample

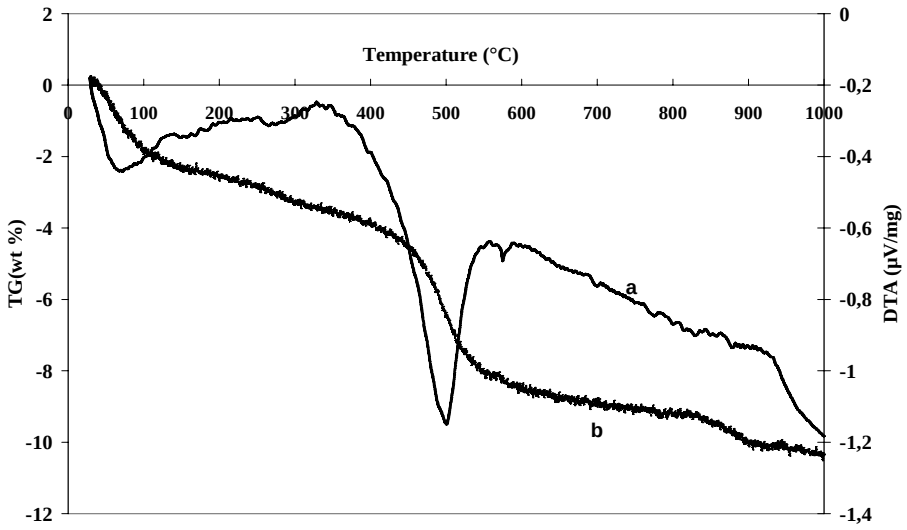

Figure 6: Thermal analyses of sample: a: DTA curve; b: TG curve

between the supports of tiles, l: the width, e: the thick)

3. Results and discussion

3.1. Geotechnical characteristics

The particle size distribution of the sample (**Fig.2**) shows that the sample is constituted of 45 wt.% of clay fraction (Φ < 2μm), 53wt.% of silt (2<Φ<60μm) and 3wt.% of sand (Φ >60μm). The clayey fraction is responsible of the raw material plasticity and silt and sand are considered non-plastics materials. The sample body presents then a mixture of plastics and non-plastics materials, and must give then a satisfactory mechanical properties and drying stage of the green pieces [8].These results are correlated with the position of the sample in the Marsigli diagram (**Fig.3**) according to the plasticity index (23.1%) and plasticity limit (48.1%). The sample is located in a region considered as optimal for extrusion.

3.2. Mineralogical composition

3.2.1. X-ray diffraction (XRD)

Powder X-ray diffraction pattern of the sample (**Fig.4)** showed that this one is mainly constituted of kaolinite and quartz as major crystallized phases and some minor phases like orthose, albite, talc and iron minerals (goethite and hematite) according to their weakness peaks intensities .

3.2.2. Infrared spectroscopy (IR)

The infrared spectrum of the sample **(Fig.5)** showed the prominent bands located at around 3696, 3653 and 3621cm^{-1} attributable to the kaolinite [10]. The two first are assigned to vibrations of outer sheet hydroxyls of kaolinite. The third one corresponds to the vibrations of inner hydroxyls localised between the tetrahedral layer Si_2O_5 and the octahedral layer $Al_2(OH)_6$. Hygroscopic water of the samples is characterized by the stretching band at around 3435cm^{-1} and the bending 1633cm^{-1} [11,12]. The bands around 912 and 930cm^{-1} correspond to Al-OH vibration [12]. This doublet is not well defined showing that the kaolinite is not well crystallized. This result is correlated by the shapes of the kaolinite 00l peak which is not so well defined. The band at 536cm^{-1} is assigned to Si-O-Al deformation. Bands at around 1035, 791 and 467cm^{-1} correspond to Si-O vibrations and could be probably assigned to quartz.

3.2.3. Thermal analysis (DTA / TG)

DTA/TG curves of the sample are presented in **Fig.6**. The DTA curve shows endothermic peaks at 90, 300, 500 and 580°C and one exothermic peak at 940°C. The TG curve indicates principally three steps of weight loss. The first at around 90°C is about 2.6wt.% and corresponds to the first endothermic peak. This peak is due to the evaporation of adsorbed water. The second weight loss around 300°C is about 1wt.% and corresponds to the second endothermic peak which corresponds to the goethite transformation into hematite[13] according to equation 1 and 2:

$$2\gamma\text{-FeOOH} \xrightarrow{255°C} \gamma Fe_2O_3 + H_2O \quad (1)$$

$$2\alpha\text{-FeOOH} \xrightarrow{279°C} \alpha Fe_2O_3 + H_2O \quad (2)$$

The following weight loss located at 500°C is around 5.52.wt.%. This weight loss, which corresponds to dehydroxylation of kaolin into metakaolin (3), is important, showing the important amount of kaolinite in the sample [14,15].

$$Si_2O_5Al_2(OH)_4 \rightarrow 2SiO_2\text{-}Al_2O_3 + 2H_2O \quad (3)$$

The dehydroxylation temperature is lower than that of well crystallised kaolinite, this proves that the kaolinite of the sample has a low cristallinity as indicated by infrared spectrometry and X-ray diffraction studies.

The peak at 580°C is assigned to the allotropic transformation of quartz α to quartz β.

Table I: Geotechnical characteristics of the samples

Properties	Results
Materials characteristics	
Colour	brown
Density (g/cm^3)	2, 72
Weight loss at 105°C (%)	2, 65
Weight loss at 1000°C (%)	7, 52
Atterberg limits	
Liquid limit, w_L (%)	48, 1
Plasticity limit, w_P (%)	25
Plasticity index I_P (%)	23, 1
Particles size distribution (wt. %)	
Clays (<2µm)	45
Silt (2<Φ<60µm)	52
Sand (>60µm)	3

Table II: Chemical composition of Kor

Oxides	Al_2O_3	SiO_2	Fe_2O_3	Na_2O	K_2O	CaO	MgO	$Ti0_2$	LOI	Total
Kor (wt. %)	20,3	57,2	6,53	1,49	2,91	0,99	1,12	0,71	7,52	98,77

Table III : Semi-quantitative mineralogical composition of the samples

Crystallized mineral	Kaolinite	Quartz	Orthose	Albite	Goethite	Hematite	Talc	Calcite	Anatase
Wt.%	37	18	17	13	4	3	4	2	1

The exothermic peak at 940°C is the transformation of metakaolin to mullite via spinel phase [16]:

$$2\,[2SiO_2\text{-}Al_2O_3] \rightarrow Si_3Al_4O_{12} + SiO_2 \quad (4)$$

The temperature of this peak is lower than that indicated by Chakraborty and Ghosh at 980°C [17]. This is due to the different impurities on the material. We noted also around 800-900°C a feeble weight loss (1wt.%) assigned to the transformation of talc to enstatite [18].

3.3. Chemical composition

The chemical composition of the sample is given in **Table 2**. The sample is constituted of important amount of SiO_2 (57.2 wt.%) associated with an appreciable amount of Al_2O_3 (20.3wt.%). The high value of Al_2O_3 and SiO_2 confirms that the sample is rich on quartz and alumino-silicate components. Iron oxide Fe_2O_3 is present in appreciable quantity (6.53wt. %) and justifies the relative feeble temperature of kaolinite dehydroxylation as showed the DTA curve. K_2O and Na_2O exist but in small quantity and confirm the presence of feldspar components.

3.4. *Semi-quantitative composition of minerals phases*

While bringing closer the results of the chemical analysis of those to the x-ray diffraction, the crystalline mineral phases percentages contained in the sample were determined according to Njopwouo's methodology [7]. **Table 3** gives the semi-quantitative mineralogical composition of the mineral phases of the sample. The sample contains principally kaolinite (37wt.%) and quartz (18wt.%). These results are correlated with the x-ray diffraction and infrared results. The studied sample contains also feldspar component such as orthose (17wt. %) and albite (13wt.%) in important quantity. They melt above 1000°C and contribute to decrease the porosity of material by forming with quartz an eutectic around 1060°C. At this temperature the material viscosity is between the solid and liquid phase [19]. The presence of talc improves the mechanical properties by cordierite formation [20]. It is also the case of calcite which can form anorthite and improve the fired products properties.

3.5. Mechanical characteristics

The feeble drying shrinkage (0.25%) is interesting because it indicates very weak risks of materials cracks during their firing. This value is correlated with the plasticity of sample and particle size. The shrinkage increase with fired temperature (**Fig.7**). This increasing of shrinkage is due to the consolidation of material during sintering. This densification confers the important mechanical resistance of tiles.

Fig.8 shows the flexural strength and water absorption of the fired tiles. At the low temperatures (950°C), the sample exhibited an interesting flexural strength (21.5MPa) corresponding to required values for fired bricks. At 1000°C, the flexural strength increase until 28.15MPa which is not far to the 30MPa required for sandstone floor tiles. With increasing the sintering temperature, flexural strength and porosity are 59.5MPa and 0.69% respectively, similar to stoneware values.

The different interesting mechanical resistance is due to the mineralogical composition. The sample contains plastics and non plastic minerals in good proportion which increase the flexural strength. The presence of talc and calcite contributed to further increase the mechanical properties.

3.6. Mineralogy of fired products

The mineralogy of fired products has been achieved by infrared spectroscopy. The results are show by the **Fig.9**. The different bands are summarized in the **Table 4**.

At 950°C, the kaolinite bands disappeared (1035.12; 912.36; 752.24cm^{-1}). This disappearing shows the dehydroxylation of all the kaolinite to

Table IV: Different infrared bands

untreated	950°C	1050°C	1150°C	Probable assignment	Reference
1035.12	1081.15	1079.36	1081.12	Si-O stretch (kaolinite-mullite)	11,12
912.36	-	-	-	Al-OH (kaolinite)	12
791.96	779.53	778.49	796.85	Si-O Quartz	11,12
752.24	-	-	-	OH translation (Kaolinite lattice)	11,12
693.84	694.42	693.99	693	Si-O Quartz	11,21
640	647.52	642.09	640	Si-O-Si bending	21
-	580.88	571.68	547.56	MgO Cordièrite	22
536.01	536.06	-	-	Si-O-Al	12
467.19	467.22	458.16	462.74	Si-O quartz Si-O-Mg Talc	11 21

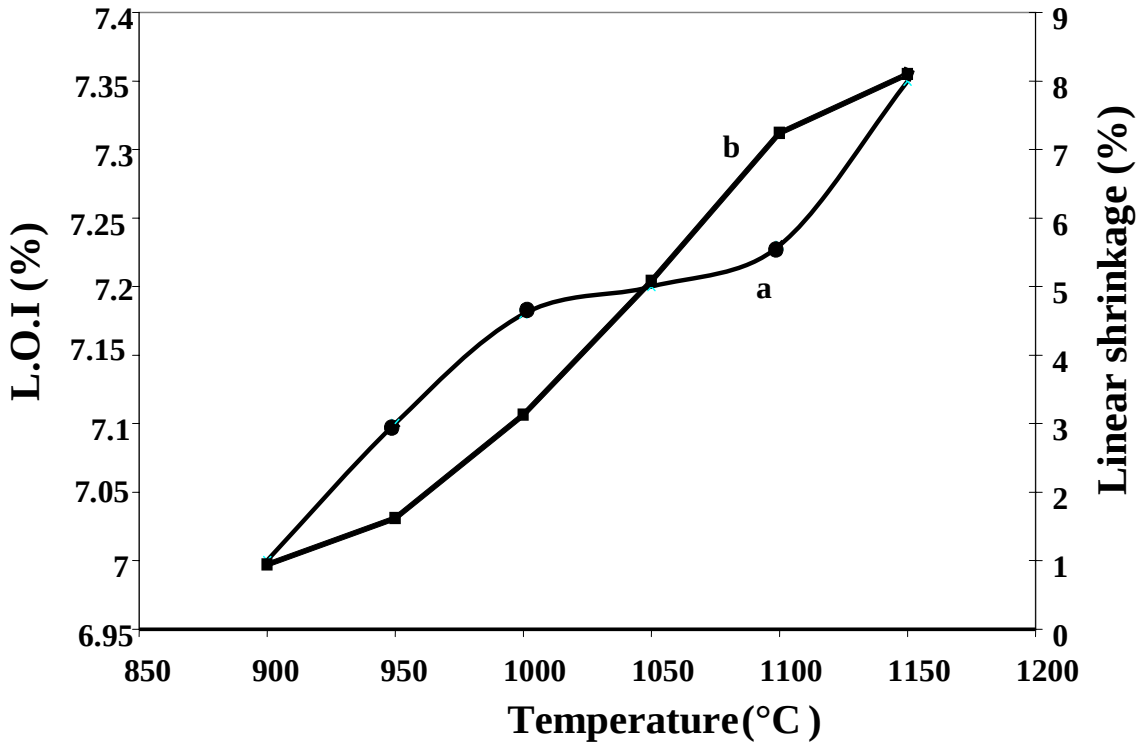

Figure 7: a: Linear shrinkage; b: Loss on ignition

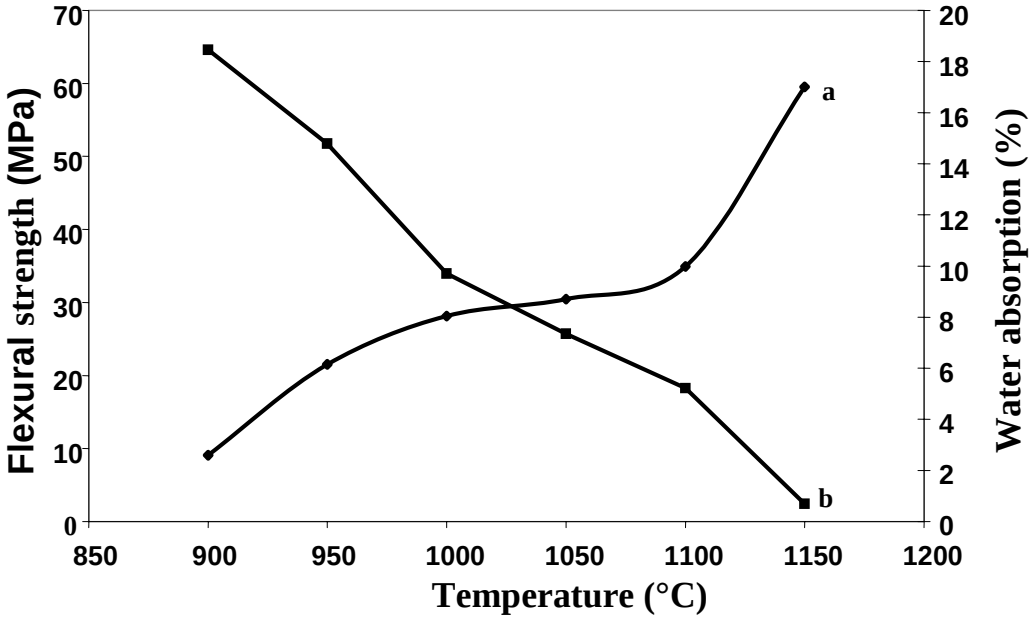

Figure 8: Evolution of flexural strength and water absorption with temperature
a: Flexural strength; b: Water absorption

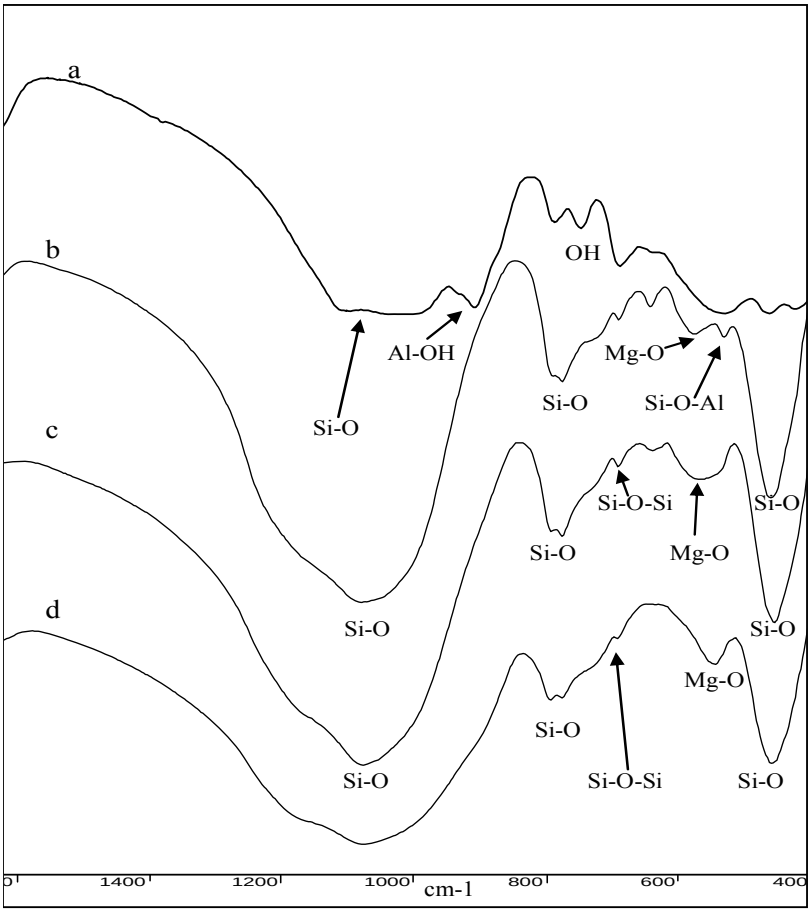

Figure 9: Infrared spectra of sintered products (low frequency)
a: untreated, b: 950°C, c: 1050°C, d:1150°C

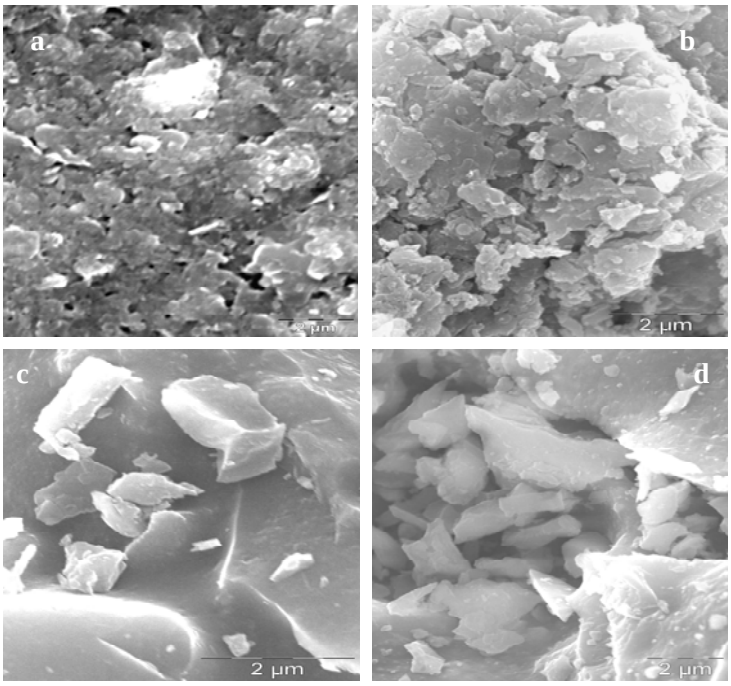

Figure 10: SEM micrographs: a- untreated; b- 900°C ; c-1100°C; d- 1150°C

metakaolinite. This metakaolinite also reorganized to mullite and/or spinel phase. The new bands located at 580.88 and 1081 cm^{-1} show respectively the formation of cordierite and mullite at 950°C. These two phases remain in the material during firing and improve the mechanical properties. The changing of frequencies during sintering is due to the structural evolution of the crystalline phase. The quartz remains in the material at the different temperature but in different crystalline form: quartz α (791cm^{-1} untreated) → quartz β (779cm^{-1}; 950°C) quartz β (779cm^{-1}; 950°C) → tridymite (796.85 cm^{-1} ; 1150°C)
New bands around 3700cm^{-1} were formed. These bands are assigned to silanol groups which play an important role in the removal of water molecules formed by recombination of Al-OH or Mg-OH to a new bond Al-O or Mg-O.

3.7. Microstructure of fired products

The sample image (**Fig.10-a**) produced by SEM show the quasi-polygonal numerous particles and kaolinite flakes. The hexagonal flakes characteristic of kaolinite are not regular. These results show that the kaolinite of the sample is not well crystallized as indicates the infrared results. The flakes are in great proportion in the sample, showing that kaolinite is the predominant phase as indicates the density and the x-rays diffraction. The quartz is detected by the aggregates. The inclusions presences are due to the goethite.

At 900°C (**Fig.10-b**) structural reorganization of the metakaolinite occurred. This reaction increases the material volume. Mullite crystals are not observable probably due to their very small quantity, on small size and they are also hidden by the amorphous structure in great quantity of the metakaolinite and the aggregates of quartz. It is at around 1100°C (**Fig.10-c**) that first crystals of mullite are observable in the forms of bar. The beginning of mullite formation favourably contribute to the mechanical resistance of fired products. At this temperature prismatic quartz is always observable. At 1150°C (**Fig.10-d**), we note a greater number of characteristic needles of mullite. This increase of mullite content explains the best mechanical resistance. The rapid formation at low temperature can be explained by the presence of

Fe^{3+} (Fe_2O_3 ~ 7%) which induces the formation of greater quantity of mullite and favors a significant shrinkage at low temperature (< 1300°C). The quantity of mullite is in relation with the mechanical properties of the fired produced. At 1150°C, crystallized silica is still visible but in pyramidal form, which corresponds to tridymite obtained from the transformation of quartz.

4. Conclusion.

Mineralogical studies conducted on the raw clayey material showed that they are constituted of important amounts of kaolinite and quartz and feeble amounts of orthose, albite, goethite, hematite, anatase, calcite and talc. The mineralogical composition of this raw material is suitable for the elaboration of ceramic products. The fired tiles elaborated with this raw material are characterized by a low porosity and high physical and mechanical properties. This is essentially due to the formation of mullite up to 1100°C. The elaborated tiles are convenient for habitats according to the standards relevant to tiles.

Bibliography

[1]. Beyon.C.A. BAMA, Etude minéralogique, cristallographique et cristallochimique d'un gisement d'argile de Koupela (Burkina Faso), Thèse de 3eme cycle de l'Université de Ouagadougou , 1998

[2] Kabré T.S., Traoré K., Blanchart P., Applied Clays Science (1998) 12, 463-477

[3] Traoré, K., Kabré, T.S., Blanchart, P., Ceramics international (2001) 27, 875-882

[4] Karfa TRAORE, Frittage à basse température d'une argile kaolinite du Burkina Faso. Transformations thermiques et réorganisations structurales, Thèse d'état, Univ.de Limoges-Ouagadougou , 2003 pp 14

[5] NF P94-057. Analyse granulométrique des sols. Méthode par sédimentations. AFNOR., Mai 1992.

[6] NF P94-051. Détermination des limites d'Atterberg., AFNOR., Mars 1993.

[7] Njopwouo, D., Orliac, M., Cah. ORSTROM, sér. Pédol., 1979 vol.XVII, n° 4, : 329-337.

[8] Abadjo, M.F, Manual sobre fabricacion de Baldosas, tejas y ladrillos, 1 ed. 2000, Terrassa Beralmar S.A.

[9] Marsigli, M., Dondi, M, L'industria dei laterizi (1997), v.46, pp. 214-222.

[10] Rouxhet P.E., Samudacheaton N., Jacobs H et Antoro., Clay minerals (1977) 12, p.171-179

[11] J, T. Kloprogge., R, L. Frost., L, Hickey., Thermochimica Acta (2000) 345,145-156

[12] Frost, R.L.,.Vassallo, A.M., Clays and clay minerals (1996), Vol.44.No.5.635-651

[13] Konan, L.K., Seil, J., Andji, J.Y.Y., Soro, N.S., Oyetola, S., Touré, A.A., et Kra, G., J.Soc.Ouest-Afr.Chim (2001) ; 011

[14] Siaka N. SORO., Influence des ions fer sur les transformations thermiques de la kaolinite, Thèse de l'université de Limoges 2003

[15] Andji, J.Y.Y., Seil, J., Touré, A.A., Kra, G., Njopwouo, D., J. Soc. Ouest-Afr. Chim (2001) 011

[16] Konan, K L., Sei, J., Soro, N.S.S., Oyetola, S., Gaillard, J.M., Bonnet, J.P., Kra, G., J. Soc. Ouest-Afr. Chim (2006) 21 ; 35-43,

[17] Chakravorty, A.K., Ghosh, D.K., Journal of the American Ceramic Society (1991), 74(6); 1404-1406

[18] Kunal, B., Jibamitra, G., The American Mineralogist (1994) 79; 692-699

[19] Levin, E.M., Robbins, C.R., McMurdie, H.F., Phase for ceramists., The American Ceramic Society Inc., (1sted.) 1964.

[20] Blanc, J.J ; La vitrification de pâtes alcalines dopées par le talc. L'industrie céramique n°802, p 104-107 ; 1986.

[21] L. Fernandez, C. Alonso, A. Hidalgo and C. Andrade., Advances in Cement Research (2005), 17, No. 1, January, 9–21

[22] Lazarev A. N. Vibrational Spectra and Structure of Silicates. Consultants Bureau, New York, 1972.